ISSN 1392 - 1207. MECHANIKA. 2007. Nr.1(63)

Influence of surface hardening on low cycle tension-compression and bending durability in stress concentration zones

M. Daunys*, A. Sabaliauskas**
**Kaunas University of Technology, Kęstučio 27, 44312 Kaunas, Lithuania, E-mail: mykolas.daunys@ktu.lt*
***Kaunas University of Technology, Kęstučio 27, 44312 Kaunas, Lithuania, E-mail: arturas.s@tf.su.lt*

1. Introduction

The most common loading mode of operating structures, mechanisms and machinery is cyclic loading, which initiates fatigue damage. This is the main damage of aircraft and space vehicles, various type engines, transport and other machinery. In most cases unexpected fatigue damage may lead up to catastrophic failures with hardly predictable outcome.

Despite the long-term investigation history of metal fatigue damage, the mentioned problems still are of great importance. At exploitation conditions some parts of modern machines and machinery are working under elastic-plastic cyclic loads. Rationally chosen materials and technology parameters are interrelated with the durability of the parts under optimal exploitation conditions. It is impossible to solve this task missing the material properties and their laws under different loading modes in periodically varying elastic plastic deformation zone.

Exploitation durability of the parts in most cases depends not on entire part, but only on the surface layer properties. One of the efficient methods to increase durability of the parts, is hardening of the surface layer, because, in the most cases, crack initiates exactly at the surface due to insufficient quality of the surface, exploitation damage or because of working environment influence. One of the methods for surface strengthening is electromechanical treatment.

In recent years, there has been rapid progress in quantum electronics, ionic and electronic emission, plasma and electrophysics processes and new methods of metal surface hardening by concentrated energy have been developed and wider practically applied. A lot of authors have been investigating the possibility to increase the durability of the parts by various methods of surface treatment. Most of these methods are rather expensive. But more simple methods also exist. One of such methods is electromechanical treatment (EMT) of the surface. Electromechanical treatment was used by V. Bagmutov, S. Markauskas, A. Jutas and others [1-5]. Electromechanically strengthened surface is influenced by concentrated thermal flow and gets deformed plastically. Such complex influence on surface is the main point of electromechanical treatment technology. A flow of concentrated heat is obtained when electrical current passes tool-part contact. Due to high amperage current (100 - 1200 A) the surface may be heated above the 900°C temperature. Surface heating and deformation produces more fine-grained microstructure of the steel. Because the process is rapid and recrystallization is not still occurring, specific fine grained hardened surface layer, i.e. “white” layer, is obtained. “White” layer consists of significantly deformed blocks, with existing structureless martensite. Electromechanically hardened layer is highly resistant to abrasive wear. Hardening by alternating current produces hardened layer of segmented macrostructure, i.e. with alternate areas of hardened and tempered steel. Such surface is characterized by good tribological properties. The surface of parts hardened by EMT is significantly harder, more wear and fatigue resistant than the surface hardened by common thermal treatment. EMT is widely applied for surface strengthening of new and renewable machine parts.

In machine parts and structural elements often stress and strain areas are distributed nonuniformly, i.e. stress (strain) concentration zones appear. Having objective to avoid stress concentration loss complicated shapes of the parts are used, optimal conditions of thermal treatment and regimes of technological parameters are used. An attempt to avoid completely stress concentration is impossible. Concentration zones appear because of shape and geometry peculiarities of structural parts. Low cycle loading investigations in stress strain concentration zones, taking into account cyclic and mechanical characteristics of the material, the shape of concentrators, the character of nominal loads and asymmetry of loading cycles, have been analyzed and discussed in [6-9] and other publications.

Three main modes of parts’ loading are known: tension-compression, bending and torsion. During tension-compression normal stresses are uniformly distributed across the entire cross-section of deformed element. Experimental technique applied for this loading mode is well analyzed and most commonly used.

Real exploitation conditions are those causing some parts of the mechanisms to experience cyclic bending. Under particular working regimes, machinery can experience momentary overloads (e.g., axle loads in carriage chassis, cantilever cranes of telphers). Because of such load, the proportional limit is exceeded, the durability of these parts may decrease, i.e. low cycle fatigue may occur.

Investigation of material low cycle loading characteristics is widely described in [9-12] and other works. The authors of mentioned works provide investigation data on uniform (tension-compression) loading of different materials under low cycle stress and strain limited loading, depending on loading levels, asymmetry of the cycle, number of cycles and temperature.

In [13, 14] works low cycle tension-compression and pure bending results are analyzed by means of experimental and analytical investigation. It investigation was determined, that low cycle strength and durability of the parts depends not only on cyclic properties of the chosen material, but also on loading mode. Because the damage, accumulated under tension-compression is accumulated in entire cross-section of the element, while under pure bend-

ing in the most deformed outer surfaces.

2. Methods and equipment of the investigation

During electromechanical hardening the surface is under the influence of concentrated thermal flow and gets deformed plastically. Such complex impact on the surface is the main point of electromechanical treatment technology. A flow of concentrated heat is obtained as current flows through the tool-part contact. Due to high amperage current (100 - 2500 A) the surface may be heated up to the temperature above 900°C. This temperature is high enough for austenitic transformation to occur. By surface heating and deformation microstructure of the steel gets especially fine grained. Because the mentioned process is rapid, recrystallization is not yet occurring and specific fine grained hardened surface layer - "white" layer is obtained. "White" layer is formed of significantly deformed blocks, with structureless martensite.

Specimens. For low cycle tension-compression and bending experiments, specimens with stress concentrators, shown in Fig. 1, have been used.

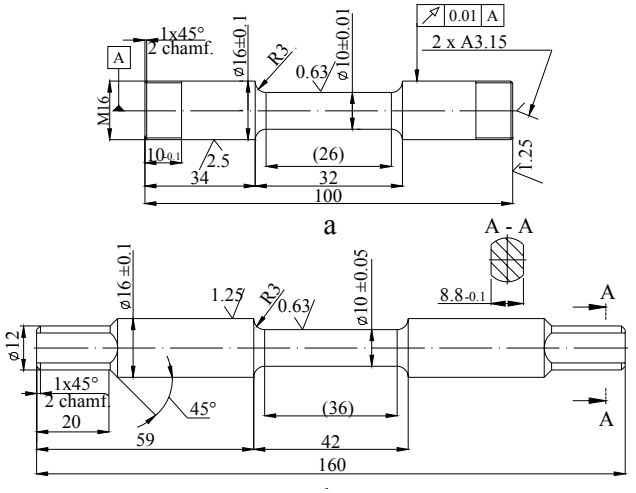

Fig. 1 Specimen with stress concentrators under low cycle loading: a - tension-compression; b - pure bending

Dimensions and shape of the hardened and non-hardened specimens were identical. To create a stress concentrator 3 mm radius was chosen where the investigated specimen has change in diameter.

Experimental setup used for EMT. Turning lathe most commonly is used for EMT, however, taking into account the surface shape, other types of machines may also be used. To obtain hardened surface, the equipment owned by Kaunas University of Technology EMT, adjusted to work on turning lathe, was used. Schematic circuit of experimental setup is shown in Fig. 2.

For electromechanical treatment of the parts universal turning lathe, together with voltage reduction transformer *3*, adjusting rheostat *2* and devices for voltage and current control and measurement were used. Current flows through the transformer *3*, which has circuit branch connected to the lathe grip *4*. Through the grip the current is transferred to the processed specimen *5*. The other branch of the circuit is attached to treatment tool *6*. It is possible to control current intensity in secondary circuit, taking

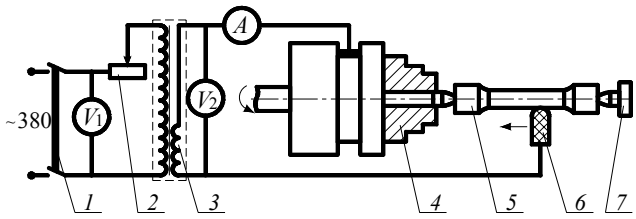

Fig. 2 Schematic circuit of EMT on turning machine: *1* - voltage switch, *2* - rheostat, *3* - voltage reduction transformer *4* - grip, *5* - specimen, *6* - special hold-down attachment for T15K6 alloy plate, *7* - toolhead

into account contact resistance of the tool and work piece, surface quality requirements and quality requirements of machined surface layer. Current amperage may vary from 100 up to 1000 A and voltage range from 0.25 up to 8 V. Furthermore, particular attachment was used for hard alloy plate pressing.

EMT regimes used to obtain "white" layer. Thickness and microhardness H_μ of the "white" layer depends on EMT regimes. The following regimes have been used for electromechanical hardening:

T15K6 hard alloy plate pressing force $F = 400$ N; specimen revolutions $n = 250$ rev/min; machining speed $v = 7.85$ m/min; tool feed rate $s = 0.11$ mm/rev; current intensity $I = 220$ A; passing number $i = 2$.

Experimental setup for static tension and low cycle tension compression. For stress and strain state investigation low frequency mechanical loading machine with electronic-mechanical strain diagrams recording apparatus have been used. Mentioned experimental setup has three basic systems: loading device, forces and strain registering apparatus and control system of the loading. To obtain static and low cycle tension-compression results 100 kN tension-compression testing machine designed at KTU was used.

Experimental setup for low cycle pure bending. Experimental investigation of low cycle pure bending was accomplished using the same above described experimental setup. However, the grip of tension-compression machine was equipped with bended specimen fixing device. General view of the mentioned device is given in [15].

FEM simulation. 3D FE models were developed, taking into account dimensions of specimens presented in Fig. 1. For the development of models it is possible to choose FE of different type. Therefore, taking into account computer hardware resources, *Solid95* type FE (Fig. 3) was used for our model development.

ANSYS FEM software was employed for development of double-layer (core of grade 45 steel and outer "white" layer) 3D numerical models of structural element. To perform calculations, mechanical properties of the core have been chosen from the data obtained during the static tension experiments of grade 45 steel, whereas outer "white" layer - from analytical calculation data presented by A. Jutas [3]. According to the same calculation data the thickness of hardened "white" layer was taken equal to 50 μm. Mechanical properties of the model layers are presented in Table 1.

Two 3D models for ¼ part of the specimen working area were developed to simulate the tension, i.e. model for grade 45 steel with core mechanical properties and lay-

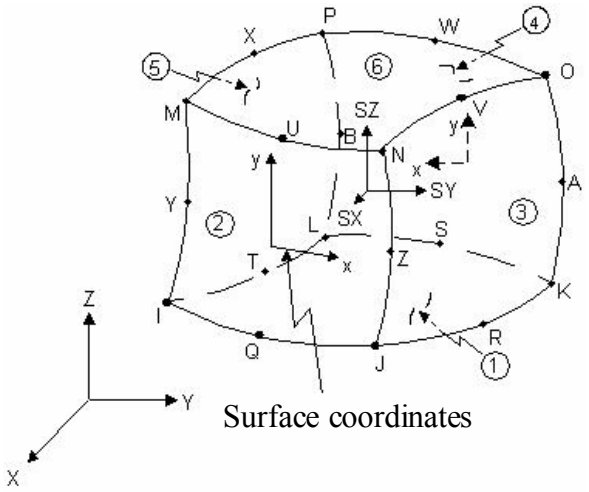

Fig. 3 *Solid95* type FE

Table 1

Mechanical properties of the materials used in numerical model

σ_{pr}, MPa	R_m, MPa	σ_f, MPa	e_{pr}, %	e_u, %	Z,%
Grade 45 steel (core)					
375	786	882.5	0.22	29	28
Outer "white" layer					
709	2033	2033	0.355	4.4	4

ered model for the hardened grade 45 steel. The model for hardened grade 45 steel consists of grade 45 steel core and outer "white" layer shell. FE mesh was refined in the zones of stress-strain concentration. FE meshing of this model is shown in Fig. 4.

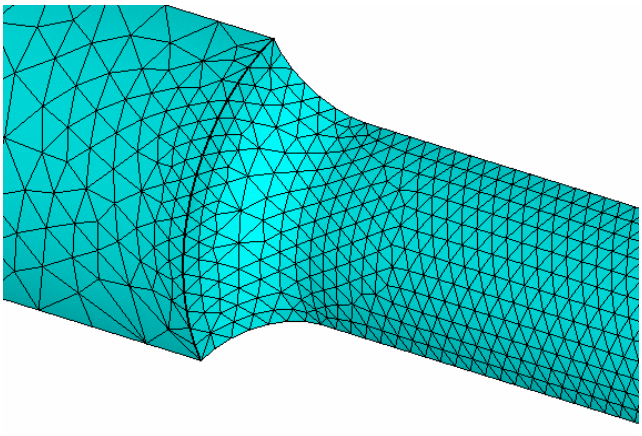

Fig. 4 FE model meshing for tension bar with concentrator

Solving the model, horizontal bottom area was constrained along the *Y* axis direction, front vertical - along the *Z*, and left end - along the *X* axis direction. Near the right end-surface distributed tensile load was applied along the perimeter. Stress and strain concentration factors have been calculated by FEM under the conditions as nominal stress $\overline{\sigma}_{in}$ in net cross-section corresponds to 0.2, 0.3, 0.4, 0.5, 0.6, 0.7, 0.8, 0.9, 1.0, 1.05, 1.1, 1.2, 1.3, 1.4, 1.5, 1.6, 1.7, 1.8 of proportionality limit for grade 45 steel. Calculations were performed for the model with and without the hardened layer.

For the case of pure bending two FE models have been also developed (for hardened and nonhardened steel), corresponding to ½ of the specimen's working area. FE mesh was refined on entire surface of "white" layer. The model is shown in Fig. 5.

During the model calculation, smaller in diameter end was constrained along the *X*-axis. Moreover, point support was attached to the higher diameter end, thus constraining displacement along the *Y* axis. At the higher in diameter end, according to pure bending loading scheme, a force was applied, which creates such bending moment M_b, that nominal stress $\overline{\sigma}_{in}$ in net cross-section corresponds to 0.2, 0.3, 0.4, 0.5, 0.6, 0.7, 0.8, 0.9, 1.0, 1.05, 1.1, 1.2, 1.3, 1.4, 1.5, 1.6, 1.7, 1.8 of grade 45 steel proportionality limit. Calculations have been made for the model with the hardened layer and without the hardened layer.

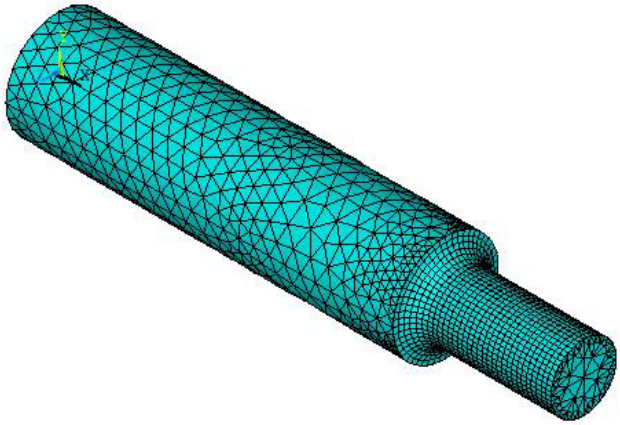

Fig. 5 FE model meshing for bending bar with concentrator

At simulation the number of elements and the element size near the stress concentrator were varied, afterwards, the obtained results were analyzed. When the difference in results was nonsignificant, a conclusion was made, that chosen mesh suits well for further calculations. FE mesh was generated providing side length of the element. Element side near the rounding radius was refined up to $2h$ (here $h = 50\ \mu m$ is thickness of the hardened layer). Whereas along the entire "working" length of the specimen, element side length was equal $30h$, while for nonhardened areas - $50h$.

Stress distribution in the zones of concentration is given in Fig. 6.

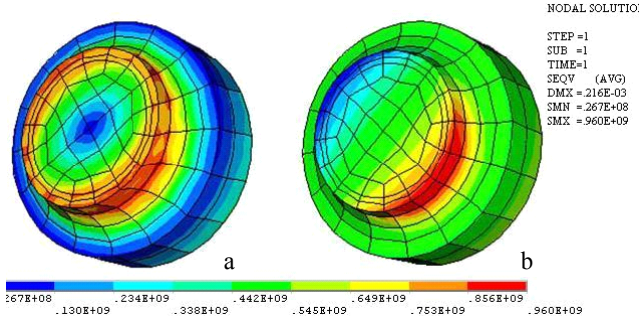

Fig. 6 Stress distribution in the zones of concentration under tension (a) and bending (b)

3. Research of low cycle loading parameters under uniaxial stress state

3.1. Results of strain limited low cycle loading

Substitution of varying cyclic plastic strain δ in Coffin's equation by constant value of total elastic plastic strain amplitude ε under the stress limited loading, results [16]

$$\varepsilon N_c^{m_1} = C_1 \tag{1}$$

Under the low cycle strain controlled tension-compression loading, the number of cycles up to crack initiation N_c was determined. This zone of durability is important, because after crack initiation stresses and strains are changing nonstationary and their influence on crack propagation is indefinable by the same laws. Therefore, in this work, damage accumulated of grade 45 steel and grade 45 after EMT under tension-compression, was compared and damage analysis performed only in N_c area, and in further investigations Eq. (1) constants C_1 and m_1 were used only to describe fatigue processes up to crack initiation.

Experimental results of low cycle durability and fatigue curves for grade 45 and grade 45 steel after EMT in coordinates $\lg\bar{\varepsilon} - \lg N_c$ (when $\bar{\varepsilon} = 2\bar{e}_0$) are presented in the Fig. 7.

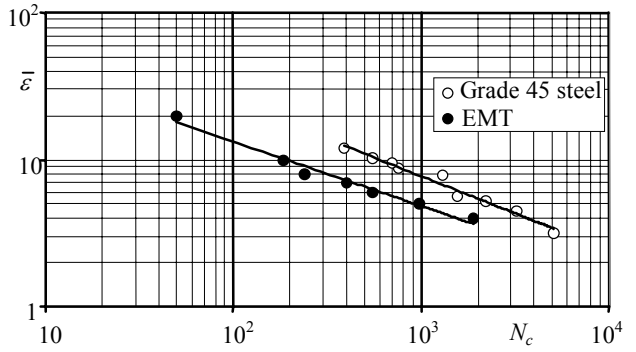

Fig. 7 Low cycle fatigue curves in logarithmic coordinates $\lg\bar{\varepsilon} - \lg N_c$, under strain controlled tension-compression

Specimens of grade 45 steel after EMT at all investigated loading levels ($\bar{\varepsilon} = 4 - 20$) show lower durability if compared to grade 45 steel specimens. Negative influence on durability of electromechanically treated steel is because of significantly small durability of hardened layer at medium to high loading levels.

3.2. Results of stress limited low cycle loading

Grade 45 steel under stress limited loading has all three types of damage: quasi-static, transitional and fatigue mode. By the experimental fatigue results, fatigue curves were formed. They are given in Fig. 8. *1*, *2* curves represent tension-compression of grade 45 steel and grade 45 steel after EMT and curves *3* and *4* show low cycle durability under pure bending. Quasi-static damage of grade 45 steel under tension-compression starts as stress amplitude is above the value $\bar{\sigma}_{\max} = 1.94$ and lasts up to N_c = 40. The area of transitional damage falls into the range between N_c = 40 and 600. Fig. 8 shows, that in this reduction of area Z (curve *5*) varies from 28% to 5%. When durability exceeds N_c = 600, only fatigue damage is evident. The mentioned damage occurs under the stresses $\bar{\sigma}_{\max} < 1.25$. While for grade 45 steel after EMT damage mode change occurs earlier. So quasi-static damage occurs under the stress amplitudes above the value $\bar{\sigma}_{\max} = 1.95$ and lasts only up to N_c = 20. In quasi-static damage zone grade 45 steel after EMT experiences damage significantly faster. This fact depends on the core (grade 45 steel) strain, therefore "white" layer cracks and causes more rapid damage of grade 45 steel after EMT. The area of transitional damage falls into the range between N_c = 20 and 400. Reduction of area Z (curve *6*) varies from 19% to 3%. Fatigue damage occurs when durability is above the value N_c= = 400 and stress is $\bar{\sigma}_{\max} < 1.3$. From this loading level the durability of the hardened specimen is higher than the durability of nonhardened grade 45 steel specimens.

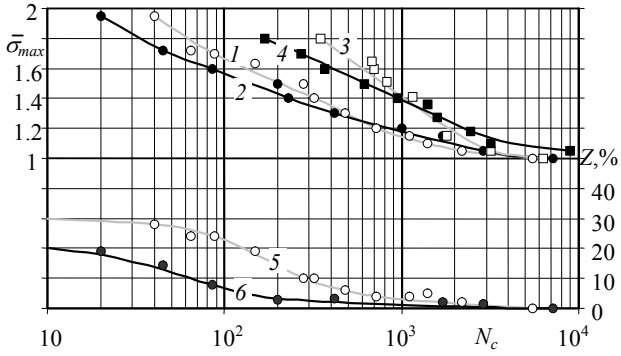

Fig. 8 Experimental curves of low cycle fatigue for nonhardened (curves *1,3,5*) and hardened specimens (curves *2,4,6*) (*1,2* - under tension-compression; *3,4* - under bending)

Under pure bending, durability significantly increases, because elastically deformed core of the specimen prevents accumulation of plastic strain in tension direction. However, like in tension-compression case, the durability of hardened specimens under high level loading is smaller than the durability of nonhardened steel specimens (here, as $\bar{\sigma}_{\max} > 1.3$ and higher). Similarly, like in tension-compression case, when $\bar{\sigma}_{\max} < 1.3$, hardened layer is able to prevent plastic deformation of the core. Because the main part of the specimen volume is the core, therefore strain of the core predetermines durability of the specimen.

Main advantage of the hardened layer is prevention of core plastic deformations.

3.3. Determination of accumulated low cycle damage

Under low cycle stress limited loading, material is always accumulating quasi-static d_K and fatigue d_N damage. The sum of mentioned damage predetermines durability of the parts. Total damage of the material is written by the dependence

$$d_N^q + d_K^l = 1 \tag{2}$$

Quasi-static damage is calculated by the dependence

$$d_K = \frac{\bar{e}_{pk}}{\bar{e}_u} \tag{3}$$

and fatigue damage by

$$d_N = \frac{\bar{\delta}_k}{\sum_1^{k_N} \bar{\delta}_k} \tag{4}$$

here $\bar{e}_u$ is uniform strain under monotonic loading, k_N is theoretical number of semicycles up to crack initiation, for any level of stress limited loading considering that $d_K = 0$ at this level [16].

Therefore, to calculate fatigue damage d_N under stress limited loading, it is necessary to have the theoretical low cycle fatigue curves, representing only fatigue damage. Determining these curves makes possible to consider stress limited loading as nonstationary strain limited loading. Then

$$\frac{\bar{\delta}_1 \bar{\varepsilon}_1^{m_3}}{C_2 C_3^{m_3}} + \frac{\bar{\delta}_2 \bar{\varepsilon}_2^{m_3}}{C_2 C_3^{m_3}} + \frac{\bar{\delta}_3 \bar{\varepsilon}_3^{m_3}}{C_2 C_3^{m_3}} + \ldots + \frac{\bar{\delta}_{k_c} \bar{\varepsilon}_{k_c}^{m_3}}{C_2 C_3^{m_3}} = 1 \tag{5}$$

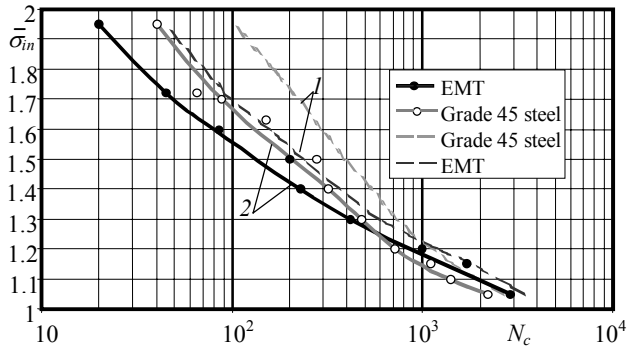

Fig. 9 Analytical (*1*) and experimental (*2*) fatigue curves for nonhardened and hardened specimens

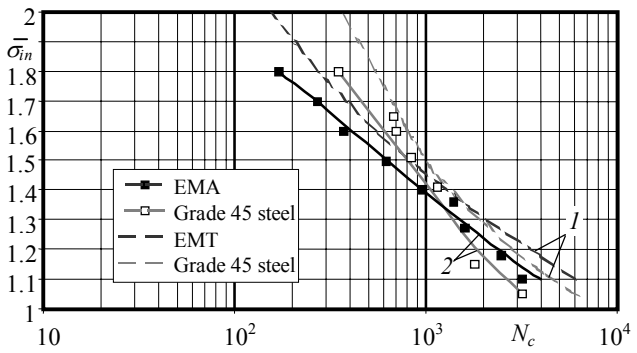

Fig. 10 Analytical (*1*) and experimental (*2*) fatigue curves for nonhardened and hardened specimens under pure bending loading

Analytical curves of the symmetric low cycle loading calculated by Eqs. (2)-(5) for grade 45 steel and grade 45 steel after EMT under stress limited loading, when only fatigue damage d_N is taken into account, are given in Figs. 9 and 10.

In Fig. 11, a, the relationship between quasi-static and fatigue damage under tension-compression, and in Fig. 11, b - under pure bending is given.

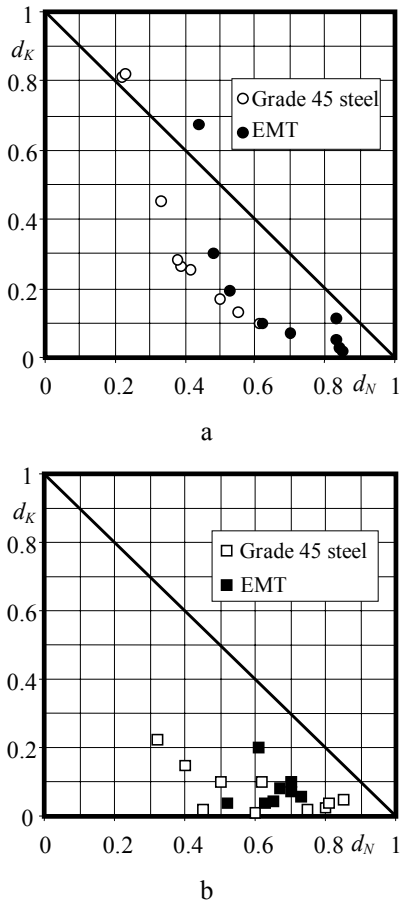

Fig. 11 Relationship between quasi-static and fatigue damage: a - under tension-compression, b - under pure bending

4. Results of experimental and analytical investigation of low cycle tension-compression and pure bending in concentration zones

Loads, due to complex geometry of the parts, cause uneven stress and strain distribution, i.e. the appearance of stresses and strains concentration zones. Under static load it is possible to neglect the influence on parts strength of local stress and strain in concentration zone. However, if a part is under cyclically varying loads, cyclic stress initiates crack formation in stress concentration zones. Therefore, part design aims to eliminate such possible areas of stress concentration. This is not always avoidable, because of parts' shape/geometry, which depends on functional purpose and manufacturing technology. But such elements significantly reduce fatigue durability being the result of stress concentration. It is known, that 80-90% of failure occurs because of fatigue damage and 90% of the damage is because of stress concentrators in parts zones. Therefore, one of the most important factors that must be taken into account while evaluating durability of the parts

under cyclic loading is stress concentration.

4.1 Calculation of concentration coefficients

Local stresses are predetermined by the shape of the part and usually are defined by the methods of elasticity theory. The main factor of local stresses is the theoretical stress concentration coefficient

$$\alpha_\sigma = \frac{\sigma_{max}}{\sigma_{nom}} \tag{6}$$

To determine stress strain state in concentration zones under elastic-plastic deformation it is necessary to use three parameters: stress concentration coefficient α_σ of elastic zone and both stress concentration coefficient K_σ and strain concentration coefficient K_e for elastic-plastic zone. N. Machutov [10] proposed an expression for the evaluation of stress concentration by theoretical stress concentration coefficient, the level of nominal stress and material stress strain curve

$$\frac{K_\sigma K_e}{\alpha_\sigma} = F\left[\alpha_\sigma, \bar{\sigma}_n, f\left(\sigma, e\right)\right] \tag{7}$$

Applying N. Machutov Eq. (7), the following is obtained

$$K_\sigma = \frac{\alpha_\sigma^{\frac{2m_0}{1+m_0}} \bar{\sigma}_{in}^{\frac{m_0-1}{m_0+1}}}{\left(\alpha_\sigma \bar{\sigma}_{in}\right)^{n\frac{1-m_0}{1+m_0}[1-(\bar{\sigma}_{in}-1/\alpha_\sigma)m_0]}} \tag{8}$$

and

$$K_e = \frac{\alpha_\sigma^{\frac{2}{1+m_0}} \bar{\sigma}_{in}^{\frac{1-m_0}{1+m_0}}}{\left(\alpha_\sigma \bar{\sigma}_{in}\right)^{n\frac{1-m_0}{1+m_0}[1-(\bar{\sigma}_{in}-1/\alpha_\sigma)]}} \tag{9}$$

when $\bar{\sigma}_{in} \le 1$, and

$$K_\sigma = \frac{\alpha_\sigma^{\frac{2m_0}{1+m_0}}}{\left(\alpha_\sigma \bar{\sigma}_{in}\right)^{n\frac{1-m_0}{1+m_0}[1-(\bar{\sigma}_{in}-1/\alpha_\sigma)]m_0}} \tag{10}$$

$$K_e = \frac{\alpha_\sigma^{\frac{2}{1+m_0}}}{\left(\alpha_\sigma \bar{\sigma}_{in}\right)^{n\frac{1-m_0}{1+m_0}[1-(\bar{\sigma}_{in}-1/\alpha_\sigma)]}} \tag{11}$$

when $\bar{\sigma}_{in} > 1$.

Equations of N.Machutov were modified by E.Z.Stowell [16] and G.Glinka [17], however, subsequent works showed, that their dependences are less precise. Therefore in subsequent our calculation Eqs. (8)-(11) were used.

FE models for bars with stress concentrators and theoretical stress concentration coefficients α_σ =1.46 for tension-compression and α_σ =1.32 for pure bending in chapter 2 were made. Values of these coefficients 1.48 and 1.34 accordingly by FEM were obtained. Coefficients of elastic-plastic loading K_e and K_σ calculated by analytical and FE methods are shown in Figs. (12), (13) and Tables 2, 3.

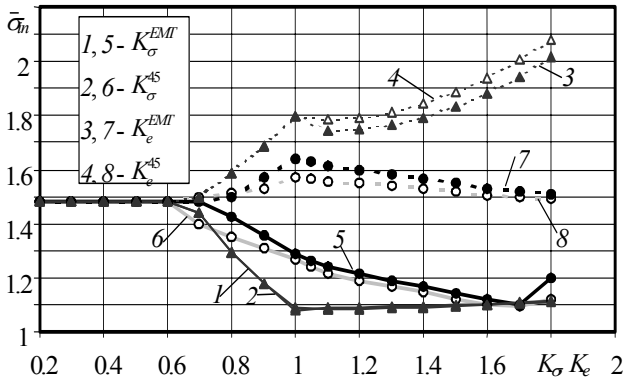

Fig. 12 Dependence of stress and strains concentration coefficients on $\bar{\sigma}_{in}$ under tension-compression, when $\alpha_\sigma^{FEM} = 1.48$ (*1 - 4* by N. Machutov, *5 - 8* by FEM)

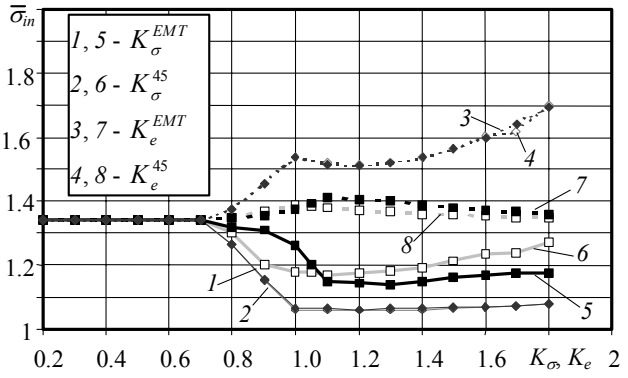

Fig. 13 Dependence of stress and strains concentration coefficients on $\bar{\sigma}_{in}$ under pure bending, when $\alpha_\sigma^{FEM} = 1.34$ (*1 - 4* by N. Machutov, *5 - 8* by FEM)

Table 2

Concentration coefficients for tension

$\bar{\sigma}_{in}$	α_σ^{FEM}	Grade 45 steel		Grade 45 steel (FEM)		EMT		EMT (FEM)	
		K_σ	K_e	K_σ	K_e	K_σ	K_e	K_σ	K_e
		m_0 = 0.142				m_0 = 0.148			
0.7	1.48	1.439	1.500	1.421	1.501	1.439	1.500	1.480	1.480
0.8		1.293	1.589	1.350	1.515	1.295	1.588	1.423	1.501
0.9		1.179	1.689	1.311	1.533	1.178	1.686	1.355	1.570
1.0		1.087	1.799	1.266	1.572	1.081	1.794	1.289	1.637
1.1		1.085	1.788	1.215	1.558	1.089	1.745	1.240	1.615
1.2		1.086	1.793	1.191	1.552	1.090	1.748	1.216	1.595
1.3		1.088	1.812	1.168	1.541	1.092	1.764	1.189	1.581
1.4		1.091	1.843	1.149	1.530	1.094	1.793	1.171	1.568
1.5		1.094	1.885	1.122	1.521	1.098	1.832	1.143	1.552
1.6		1.099	1.939	1.099	1.505	1.102	1.882	1.121	1.531
1.7		1.104	2.004	1.093	1.501	1.108	1.943	1.102	1.520
1.8		1.11	2.08	1.120	1.497	1.114	2.015	1.201	1.511

Table 3

Concentration coefficients for bending

$\overline{\sigma}_{in}$	α_σ^{FEM}	Grade 45 steel		Grade 45 steel (FEM)		EMT		EMT (FEM)	
		K_σ	K_e	K_σ	K_e	K_σ	K_e	K_σ	K_e
		m_0 = 0.142				m_0 = 0.148			
0.8	1.34	1.267	1.377	1.3	1.353	1.268	1.377	1.32	1.351
0.9		1.154	1.453	1.2	1.365	1.156	1.452	1.26	1.377
1.0		1.063	1.538	1.181	1.391	1.066	1.535	1.2	1.393
1.1		1.061	1.519	1.172	1.385	1.064	1.517	1.15	1.411
1.2		1.061	1.514	1.174	1.381	1.063	1.512	1.145	1.405
1.3		1.061	1.521	1.182	1.372	1.064	1.519	1.141	1.401
1.4		1.063	1.538	1.194	1.365	1.066	1.536	1.15	1.391
1.5		1.066	1.565	1.212	1.361	1.068	1.562	1.16	1.380
1.6		1.069	1.601	1.235	1.356	1.072	1.598	1.17	1.372
1.7		1.073	1.616	1.242	1.352	1.076	1.642	1.175	1.365
1.8		1.078	1.699	1.271	1.350	1.081	1.695	1.176	1.361

The difference between stress and strains concentration coefficients K_σ and K_e calculated by analytical and FE methods increases at increased level of loading. This difference is larger for strain concentration coefficients K_e. Coefficients calculated by FEM at subsequent calculations of stress and strains in concentration zones were used.

4.2. Investigation of low cycle loading in concentration zones

Under low cycle loading for the zone of stress concentration the following would be written [16]

$$\overline{S}_{ik} = \overline{S}_{ink} K_{Sk} \tag{12}$$

$$\overline{\varepsilon}_{ik} = \overline{\varepsilon}_{ink} K_{\varepsilon k} \tag{13}$$

Calculating K_{Sk} and $K_{\varepsilon k}$ the mentioned above dependencies were used, but static stress $\overline{\sigma}$ is replaced with the cyclic $\overline{S}$, static strain $\overline{e}$ -with $\overline{\varepsilon}$ and strengthening coefficient of static tension curve m_0 is replaced with m_k. For cyclically nonstable materials low cycle loading curves for every loading semicycle would be different, therefore, K_{Sk}, $K_{\varepsilon k}$ and m_k would also be different.

The strengthening coefficient of exponential approximation m_k is defined by the dependence [12]

$$\overline{S}_{ik} = \overline{\varepsilon}_{ik}^{\,m_k} \tag{14}$$

then

$$m_k = \frac{lg\,\overline{S}_{ik}}{lg\,\overline{\varepsilon}_{ik}} \tag{15}$$

or

$$m_k = \frac{lg\,\overline{S}_{ik}}{lg\left[\dfrac{A_{1,2}}{\overline{s}_T}\left(\overline{e}_0 - \dfrac{\overline{s}_T}{2}\right)F(k) + \overline{S}_{ik}\right]} \tag{16}$$

Cyclic parameters and coefficients are nonstable, because they depend both on loading level and on the number of semicycles. Cyclic plastic strain intensity (width of the hysteresis loop) in the concentration zones was defined by the dependence [16]

$$\overline{\delta}_{ik} = \left(\overline{\varepsilon}_{ik} - \overline{S}_{ik}\right)\overline{s}_T \tag{17}$$

Calculation results of plastic strain intensity in the zones of concentration under stress limited loading are given in Figs. 14 and 15.

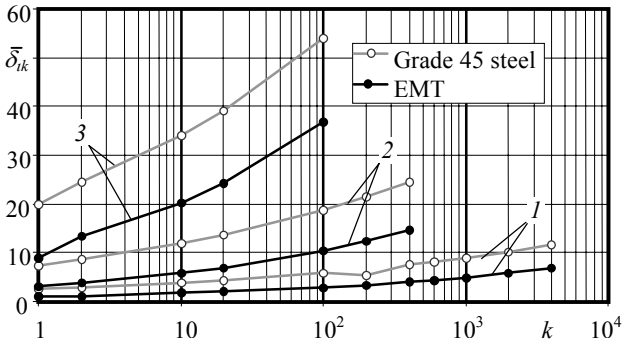

Fig. 14 Cyclic plastic strain intensity in the concentration zones at k loading semicycle under tension-compression: *1* - $\overline{\sigma}_{in} = 1.1$; *2* - $\overline{\sigma}_{in} = 1.4$; *3* - $\overline{\sigma}_{in} = 1.8$

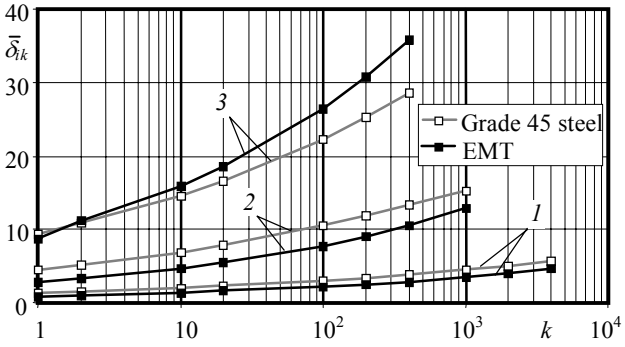

Fig. 15 Cyclic plastic strain intensity in the concentration zones at k loading semicycle under pure bending: *1* - $\overline{\sigma}_{in} = 1.1$; *2* - $\overline{\sigma}_{in} = 1.4$; *3* - $\overline{\sigma}_{in} = 1.7$

Having calculated by the Eq. (17) $\overline{\delta}_{ik}$ and known stress and strain intensities for initial loading semicycle, $\overline{\sigma}_0$ and $\overline{e}_0$, it is possible to determine the intensity of accumulated strain in tension direction $\overline{e}_{ipk}$ in the zone of concentration depending both on $\overline{\sigma}_{in}, \alpha_\sigma$ and k, under stationary nominal stress limited loading [16]

$$\overline{e}_{ipk} = \overline{e}_0 - \overline{\sigma}_0 + \sum_1^k (-1)^k \overline{\delta}_{ik} \tag{18}$$

Calculated intensity of plastic strain in tension direction in the zones of stress concentration is presented in Figs. 16 and 17.

As it is evident from Figs. 16 and 17, that plastic strain in tension direction is also accumulated in the zones of stress concentration. Under pure bending, $\overline{e}_{ipk}$ accumulation is slower than under tension.

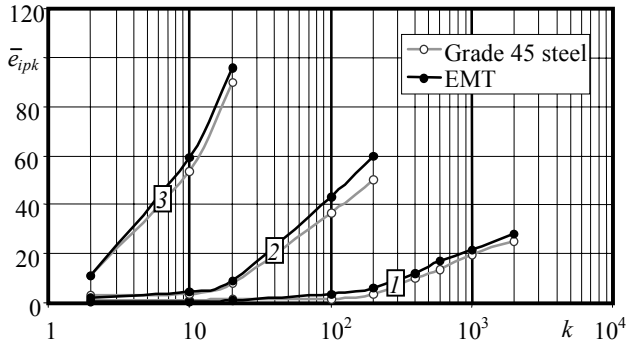

Fig. 16 Intensity of accumulated plastic strain in tension direction, in the zones of stress concentration under tension-compression: *1* - $\bar{\sigma}_{in} = 1.1$; *2* - $\bar{\sigma}_{in} = 1.4$; *3* - $\bar{\sigma}_{in} = 1.8$

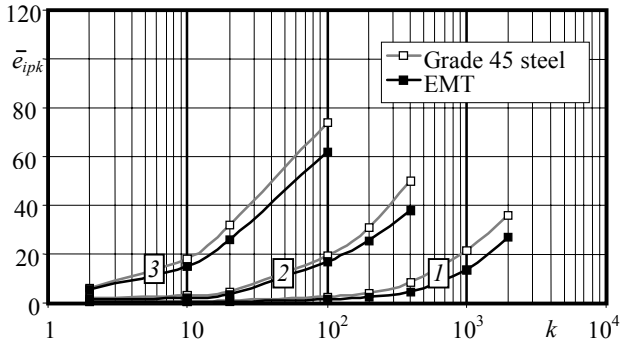

Fig. 17 Intensity of accumulated plastic strain in tension direction, in the zone of stress concentration under pure bending: *1* - $\bar{\sigma}_{in} = 1.1$; *2* - $\bar{\sigma}_{in} = 1.4$; *3* - $\bar{\sigma}_{in} = 1.7$

4.3. Investigation of damage in stress concentration zones under stress limited low cycle loading

By experimental results fatigue curves, presented in Fig. 18 have been formed. The *1* and *2* are experimental fatigue curves under tension-compression of grade 45 steel and grade 45 steel after EMT. Due to the reduce of accumulated plastic strain in tension direction at lower level of stress the resistance to damage of hardened steel is higher than that of nonhardened steel. Therefore, under low stress

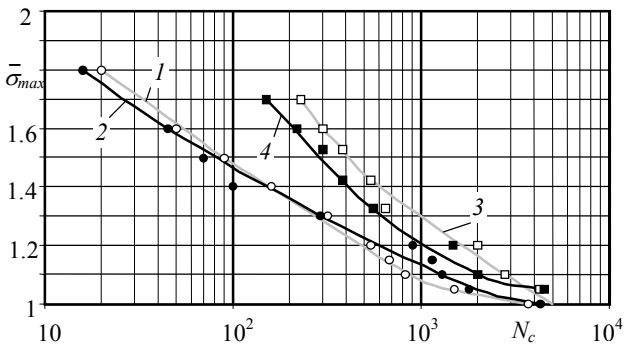

Fig. 18 Experimental curves of low cycle fatigue for nonhardened (curves *1,3*) and hardened (curves *2,4*) specimens with concentrators (*1,2* - tension-compression; *3,4* - bending)

level, electromechanically treated grade 45 steel has higher durability. This fatigue durability transformation occurs under the stress $\bar{\sigma}_{max} \le 1.3$.

The curves *3* and *4* in Fig. 18 present the data of low cycle pure bending experiments. It is evident, that under low cycle pure bending, specimens after electromechanical hardening get damaged more rapidly. And, only under loading level, which is close to proportional limit of grade 45 steel, fatigue life of the specimens made of grade 45 steel and grade 45 steel after EMT becomes equal. This could be explained stating, that stress of the "white" layer, under this loading level, is not yet exceeding proportionality limit of hardened steel.

4.4. Damage accumulation in concentration zones

Performed stress strain state analysis in the zones of concentration makes it possible to conclude, that, under stationary nominal loading, stress and strain at the zones of concentration changes nonstationary. Furthermore, at the zones of concentration under elastic plastic loading high plastic strains were obtained.

Stress strain state analysis showed, that in the zones of concentration, depending both on $\alpha_\sigma, \bar{\sigma}_{in}, \bar{e}_{in}$ mechanical and cyclic properties of the materials, the accumulation not only of fatigue damage d_N, but also quasi-static damage d_K is possible.

In this case [16]

$$d_N = \frac{\sum_1^{k_c} \frac{\bar{\delta}_{ik}}{D_e}\left(\frac{\bar{\delta}_{ik}}{D_e} + \bar{S}_{ik} s_T\right)^{m_3}}{C_2 C_3^{\,m_3}} \qquad (19)$$

and

$$d_K = \frac{\bar{e}_i - \bar{\sigma}_i + \sum_1^{k_c} (-1)^k \bar{\delta}_k}{\bar{e}_{u_2} D_e} \qquad (20)$$

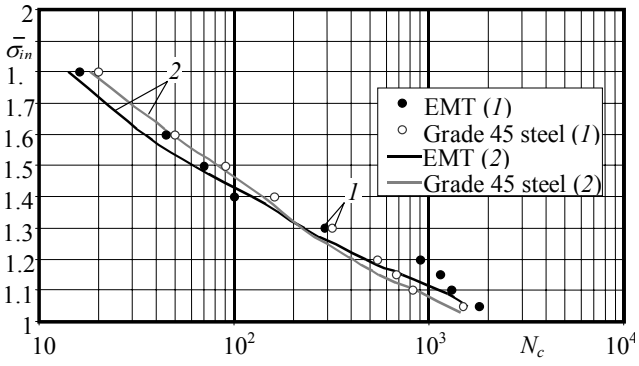

Fig. 19 Experimental results (*1*) and analytical (*2*) fatigue curves of nonhardened and hardened specimens with concentrators under tension-compression loading

Analytical curves of low cycle durability under symmetric loading, calculated by the Eqs. (1), (19) and (20), for grade 45 steel and grade 45 steel after EMT at the zones of concentration under stress limited loading, as $q = l = 0.8$, are presented in Figs. 19 and 20.

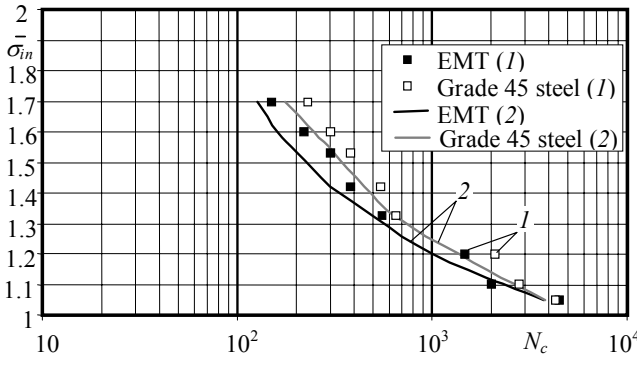

Fig. 20 Experimental results (*1*) and analytical (*2*) fatigue curves of the nonhardened and hardened specimens with concentrators under pure bending loading

From Figs. 19 and 20 is seen that the calculated durability using summation of quasi-static and fatigue damages (Eqs. (19), (20)) for tension-compression and pure bending loading are close to experimental results.

5. Conclusions

1. Under medium and low loading levels, durability of the hardened specimens increases, whereas under high loading levels EMT has negative influence on the durability. Under high level stress "white" layer cracks more rapidly and the grade steel 45 after EMT has lower durability. Because of reduced quasi-static damage at medium loading levels the durability for hardened specimens under low cycle pure bending is higher than under tension-compression.

2. It was determined, that in specimens with the stress concentration under low cycle pure bending, hardened surface has less influence on durability, when under tension-compression, while under low cycle tension-compression the positive influence starts when stress amplitude $\bar{\sigma}_{\max} \le 1.3$ value. Under pure bending accumulated plastic strain is significant lower when under tension-compression and therefore in stress concentration zones have non significant effect on durability.

3. Performed analytical investigation showed, that the suggested method for quasi-static and fatigue damage accumulation, when accumulated plastic strain and the width of the hysteresis loop are taken into account, provides a good agreement with the experimental results at stress concentration zones of surface-hardened parts under tension-compression and bending.

References

1. **Bagmutov, V., Zakharov, I.** Thermal processes modelling from effect on a material of the concentrated streams of energy.-Mechanika.- Kaunas: Technologija, 1999, Nr.4(19), p.42-49 (in Russian).
2. **Bagmutov, V., Dudkina, N., Zakharov, I.** Formation of surface layer structure produced by electromechanical strengthening of carbon steels.- Mechanika. -Kaunas: Technologija, 2005, Nr.2(52), p.55-59.
3. **Jutas, A.** Separation analysis of elastic and plastic properties on metallic specimens after using surface hardening technologies.-Mechanika, Kaunas: Technologija, 2004, No.1 (45), p.5-9.
4. **Daunys, M., Markauskas, S., Staponkus, V.** Investigation of surface quality for small diameter elements after electromechanical treatment.-Mechanika.-Kaunas: Technologija, No.1 (45), 2004, p.63-68.
5. **Barry, J., Byrne, G.** TEM study on the surface white layer in two turned hardened steels.-J. Materials Science and Engineering, 2002, v.325, No1-2, p.356-364.
6. **Machutov, N.A.** Concentration of Stresses and Strains under Elastic-Plastic Loading of Parts.-Mashinovedenije, 1971, N.6, p.54-60 (in Russian).
7. **Narvydas, E., Daunys, M.** Damage accumulation and lifetime in stress concentration zones under low cycle loading.-Mechanika.-Kaunas: Technologija 1999, No.2, p.5-8.
8. **Narvydas, E.** Modeling of damage in stress concentration zones under low cycle fatigue.-Materialpruefung, Materials Testing, v 48, n 5, 2006, p.251-255.
9. **Landgraf, R.W., Mitchell, M.R., LaPointe, N.R.**. Monotonic and cyclic properties of engineering materials. Ford motor Co., 1972. (also F. Conle, R. Landgraf, F. Richards, 1990.)
10. **Machutov, N.A.** Strain Criterion of Fracture and Strength Evaluation of Structures Elements. - Moscow: Mashinostrojenije, 1981.- 272p. (in Russian).
11. **Polak, J.** Cyclic Plasticity and Low Cycle Fatigue Life of Metals.-Elvier: Amsterdam, 1991.-316p.
12. **Daunys, M.** Strength and Fatigue Life under Low Cycle Nonstationary Loading. -Vilnius: Mokslas, 1989. -256p. (in Russian).
13. **Daunys, M., Rimovskis, S.** Analysis of circular cross-section bar, loaded by static and cyclic elastic-plastic pure bending.-Mechanika.-Kaunas:Technologija, 2002, No.1(33), p.5-10.
14. **Daunys, M., Rimovskis, S.** Analysis of circular cross-section element, loaded by static and cyclic elastic-plastic pure bending.-Int. J. of Fatigue, 2006, 28, p.211-222.
15. **Daunys, M., Sabaliauskas, A..** Influence of surface hardening on low cycle tension-compression and bending characteristics.-Mechanika.-Kaunas: Technologija, 2005, Nr.3(53), p.12-16.
16. **Daunys, M.** Cyclic Strength and Durability of Structures. -Kaunas: Technologija, 2005.-288p. (in Lithuanian).
17. **Stowell, E.Z.** The calculation of fatigue life in the presence of stress concentrations.-Nuclear Engineering and Design, 1968, v.8, No3, p.313-316.
18. **Glinka, G. and Newport, A.** Universal features of elastic notch-tip stress fields.-Int. J. of Fatigue, v.9, issue 3, July 1987, p.143-150.

M. Daunys, A. Sabaliauskas

SUKIETINTO PAVIRŠIAUS ĮTAKA MAŽACIKLIO TEMPIMO-GNIUŽDYMO IR LENKIMO ILGAAMŽIŠKUMUI ĮTEMPIŲ KONCENTRACIJOS ZONOSE

R e z i u m ė

Straipsnyje pateiktas nekietintų ir elektromechaniniu būdu sukietintų plieno 45 bandinių su koncentratoriumi, apkrautų mažacikliu tempimu-gniuždymu ir grynuo-

ju lenkimu, ilgaamžiškumo eksperimentinis ir analitinis įvertinimas. Atlikta abiem būdais apkrautų bandinių ilgaamžiškumo priklausomybės nuo apkrovimo lygio ir ciklų skaičiaus analizė. Analitiniais ir baigtinių elementų metodais atliktas įtempių ir deformacijų koncentracijos koeficientų, esant tampriai plastiniam cikliniam apkrovimui, skaičiavimas. Nustatyta, kad esant mažacikliam grynajam bandinių su koncentratoriumi lenkimui, sukietinimo paviršiaus įtaka ilgaamžiškumui yra nedidelė, o mažaciklio tempimo-gniuždymo atveju teigiamas poveikis prasideda, kai amplitudiniai įtempiai $\bar{\sigma}_{max} \le 1.3$. Analitinis tyrimas parodė, kad pasiūlytas kvazistatinių ir nuovargio pažeidimų sumavimo metodas, įvertinantis sukauptą plastinę deformaciją ir histerezės kilpos plotį, gerai tenkina eksperimento rezultatus įtempių koncentracijos zonose, esant detalių su sukietintais paviršiais tempimui-gniuždymui ir lenkimui.

M. Daunys, A. Sabaliauskas

INFLUENCE OF SURFACE HARDENING ON LOW CYCLE TENSION-COMPRESSION AND BENDING DURABILITY IN STRESS CONCENTRATION ZONES

S u m m a r y

This paper provides experimental and analytical evaluation of durability of nonhardened and hardened by EMT specimens of grade 45 steel with stress concentrators, under low cycle tension-compression and pure bending. For both types of loading modes durability analysis was carried out, taking into account fatigue and quasi-static damage depending on loading level and the number of semicycles. Stress and strain concentration coefficients were calculated by analytical and finite element methods (FEM) under elastic plastic cyclic loading. It was determined, that in specimens with the stress concentrators under low cycle pure bending, hardened surface has nonsignificant influence on the durability, while under low cycle tension-compression the positive influence starts when stress amplitude is $\bar{\sigma}_{max} \le 1.3$. The performed analytical investigation showed, that the suggested method for quasi-static and fatigue damage summation, when accumulated plastic strain and the width of hysteresis loop are taken into account, provides a very good agreement with the experimental results in stress concentration zones of surface-hardened parts under tension-compression and bending.

М. Даунис, А. Сабаляускас

ВЛИЯНИЕ УПРОЧНЕННОЙ ПОВЕРХНОСТИ НА ДОЛГОВЕЧНОСТЬ ПРИ МАЛОЦИКЛОВОМ РАСТЯЖЕНИИ-СЖАТИИ И ИЗГИБЕ В ЗОНАХ КОНЦЕНТРАЦИИ НАПРЯЖЕНИЙ

Р е з ю м е

В настоящей работе исследованы прочность и долговечность образцов из стали 45 с упрочненной поверхностью при малоцикловом растяжении-сжатии и изгибе. Проведен анализ долговечности при обоих типах нагружения в зависимости от уровня и числа циклов нагружения. Расчет коэффициентов концентрации напряжений и деформаций при упругопластическом нагружении проведен аналитическим и числовым методами. Определено, что при малоцикловом изгибе для образцов с концентрацией напряжений упрочнение поверхности оказывает незначительное влияние на долговечность. При малоцикловом растяжении-сжатии положительное влияние на долговечность проявляется при амплитудных напряжениях $\bar{\sigma}_{max} \le 1.3$. Проведенное аналитическое исследование показало, что предложенный метод суммирования усталостных и квазистатических повреждений, учитывающий накопленную пластическую деформацию и ширину петли гистерезиса, хорошо соответствует результатам эксперимента в зонах концентрации напряжений как при растяжении-сжатии, так и при изгибе.

Received January 17, 2007

DOI: 10.5755/j02.mech.14780